Determination of the Chiral Condensate from (2 + 1)-Flavor Lattice QCD

H. Fukaya,[1] S. Aoki,[2] S. Hashimoto,[3,4] T. Kaneko,[3,4] J. Noaki,[3] T. Onogi,[5] and N. Yamada[3,4]

[1]*Department of Physics, Nagoya University, Nagoya 464-8602, Japan*
[2]*Graduate School of Pure and Applied Sciences, University of Tsukuba, Tsukuba 305-8571, Japan*
[3]*KEK Theory Center, High Energy Accelerator Research Organization (KEK), Ibaraki 305-0801, Japan*
[4]*School of High Energy Accelerator Science, The Graduate University for Advanced Studies (Sokendai), Ibaraki 305-0801, Japan*
[5]*Department of Physics, Osaka University, Toyonaka 560-0043, Japan*
(Received 10 December 2009; published 25 March 2010)

We perform a precise calculation of the chiral condensate in QCD using lattice QCD with 2 + 1 flavors of dynamical overlap quarks. Up and down quark masses cover a range between 3 and 100 MeV on a $16^3 \times 48$ lattice at a lattice spacing ~ 0.11 fm. At the lightest sea quark mass, the finite volume system on the lattice is in the ϵ regime. By matching the low-lying eigenvalue spectrum of the Dirac operator with the prediction of chiral perturbation theory at the next-to-leading order, we determine the chiral condensate in (2 + 1)-flavor QCD with strange quark mass fixed at its physical value as $\Sigma^{\overline{\rm MS}}(2 \text{ GeV}) = [242(04)(^{+19}_{-18}) \text{ MeV}]^3$ where the errors are statistical and systematic, respectively.

Spontaneous breaking of chiral symmetry is one of the most fundamental properties of quantum chromodynamics (QCD), as it produces the bulk of the hadron masses. The symmetry breaking is indicated by a nonzero value of the chiral condensate Σ, which is an expectation value of the scalar density operator $\bar{q}q$. Despite its importance, calculation of Σ remains a significant challenge, even using the numerical simulation of QCD on the lattice, due to both ultraviolet and infrared problems.

On the ultraviolet side, an additive renormalization of the scalar operator diverges as $\sim 1/a^3$ as the lattice spacing a decreases, when the chiral symmetry is violated. Even with exact chiral symmetry, there exists a quadratic divergence proportional to the quark mass. On the infrared side, since spontaneous symmetry breaking does not occur at finite volume, the infinite volume limit has to be taken before going to the massless limit. Therefore, careful study of the scaling in the chiral and infinite volume limits is crucial to determine Σ.

Our previous work [1,2] opened a new possibility to overcome these difficulties by performing a lattice QCD employing the overlap fermion formulation [3,4], which preserves exact chiral symmetry at finite lattice spacings. The ultraviolet problem is avoided by using the spectrum of low-lying fermion modes. According to the Banks-Casher relation [5], the spectral density $\rho(\lambda)$ of the Dirac operator at $\lambda = 0$ is related to the chiral condensate as $\Sigma = \pi\rho(0)$. At a large but finite volume V, chiral perturbation theory (ChPT) can be used to predict the volume scaling of the near-zero modes, which is also equivalently described by the chiral random matrix theory [6–9]. By matching the theoretical prediction with the lattice data, the chiral condensate Σ was determined at the leading order (LO) in the ϵ expansion (see also [10]).

This Letter extends the previous work in several directions. (i) Based on a new ChPT calculation by Damgaard and Fukaya [11], which is valid in the conventional p regime as well as in the ϵ regime, we use the lattice data at several values of sea quark masses. (ii) The new formula consistently treats the next-to-leading order (NLO) effects in the p expansion and thus, the result of Σ has the NLO accuracy (A similar NLO analysis of the lattice data taken with the Wilson fermion in the p regime has been done recently [12].). (iii) The lattice data are newly generated including the effect of strange quark, so that the result corresponds QCD in nature. (iv) The finite volume scaling is confirmed using two volumes $16^3 \times 48$ and $24^3 \times 48$. With these new developments, the determination of Σ is made more precise and reliable.

The spectral density at a given topological charge Q is calculated within ChPT at NLO as [11]

$$\rho_Q(\lambda) = \Sigma_{\rm eff}\hat{\rho}_Q^\epsilon(\lambda\Sigma_{\rm eff}V, \{m_{\rm sea}\Sigma_{\rm eff}V\}) + \rho^p(\lambda, \{m_{\rm sea}\}), \quad (1)$$

for an eigenvalue λ of the Dirac operator. Assuming the analyticity, $\rho_Q(\lambda)$ is obtained through the real part of the chiral condensate with a valence quark mass equal to an imaginary value $i\lambda$. Here $\Sigma_{\rm eff}$ is an "effective" chiral condensate of which definition is given below.

The spectrum of the near-zero quark modes ($\lambda \sim 1/\Sigma V$) is mainly affected by the zero-momentum pion modes. In fact, the first term in (1) is the same as the spectral density at the leading order of the ϵ expansion [6–9] expressed as a function of dimensionless combinations $\lambda\Sigma_{\rm eff}V$ and $\{m_{\rm sea}\Sigma_{\rm eff}V\} = \{m_1\Sigma_{\rm eff}V, \cdots, m_{N_f}\Sigma_{\rm eff}V\}$ expressed by

$$\hat{\rho}_Q^\epsilon(\zeta, \{\mu_{\rm sea}\}) \equiv C_2 \frac{|\zeta|}{2\prod_f^{N_f}(\zeta^2 + \mu_f^2)} \frac{\det\tilde{\mathcal{B}}}{\det\mathcal{A}}, \quad (2)$$

with $N_f \times N_f$ matrix $\mathcal{A}$ and $(N_f + 2)(N_f + 2)$ matrix $\tilde{\mathcal{B}}$ defined by $\mathcal{A}_{ij} = \mu_i^{j-1}I_{Q+j-1}(\mu_i)$ and $\tilde{\mathcal{B}}_{1j} = \zeta^{j-2}J_{Q+j-2}(\zeta)$, $\tilde{\mathcal{B}}_{2j} = \zeta^{j-1}J_{Q+j-1}(\zeta)$, $\tilde{\mathcal{B}}_{ij} = (-\mu_{i-2})^{j-1}I_{Q+j-1}(\mu_{i-2})$ ($i \neq 1, 2$), respectively (J_k's

and I_l's denote the (modified) Bessel functions.). The phase factor C_2 is 1 for $N_f = 2$ or 3.

The second term in (1) is the NLO correction seen in the ordinary p-expansion [13]. With the meson mass $M_{ij}^2 \equiv (m_i + m_j)\Sigma/F^2$, which is made of either sea quark (f) or valence quark (v), it is expressed as

$$\rho^p(\lambda, \{m_{\mathrm{sea}}\}) \equiv -\frac{\Sigma}{\pi F^2} \mathrm{Re}\Bigg[\sum_f^{N_f} \Big(\bar{\Delta}(M_{fv}^2) - \bar{\Delta}\Big(\frac{M_{ff}^2}{2}\Big) \Big)$$
$$- (\bar{G}(M_{vv}^2) - \bar{G}(0)) \Bigg]\Big|_{m_v = i\lambda}. \quad (3)$$

The function $\bar{\Delta}(M^2)$ contains the chiral logarithm, $\bar{\Delta}(M^2) = \frac{M^2}{16\pi^2}\ln\frac{M^2}{\mu_{\mathrm{sub}}^2} + \bar{g}_1(M^2)$, with $\bar{g}_1(M^2)$ representing the finite volume effect [14]. The subtraction scale μ_{sub} is set at 770 MeV in this work. The other function $\bar{G}(M^2)$ has a double-pole contribution due to the partial quenching. The explicit forms of $\bar{g}_1(M^2)$ and $\bar{G}(M^2)$ are given in [11] [In this Letter, we use a simplified notation. $\bar{G}(M^2)$ corresponds to $\bar{G}(0, M^2, M^2)$ in [11]]. The effective chiral condensate Σ_{eff} in (1) is given by

$$\Sigma_{\mathrm{eff}} = \Sigma\Bigg[1 - \frac{1}{F^2}\Big(\sum_f^{N_f} \bar{\Delta}\Big(\frac{M_{ff}^2}{2}\Big) - \bar{G}(0) - 16L_6^r \sum_f^{N_f} M_{ff}^2 \Big) \Bigg], \quad (4)$$

where L_6^r (renormalized at μ_{sub}) is one of the low-energy constants at NLO [15].

Numerical simulations of lattice QCD are performed using the Iwasaki gauge action at $\beta = 2.3$ including $2 + 1$ flavors of dynamical overlap quarks on a $16^3 \times 48$ lattice. The lattice spacing $a = 0.1075(7)$ fm is determined from the heavy quark potential with an input $r_0 = 0.49$ fm. For the strange quark mass, we choose two different values $m_s = 0.080$ and 0.100 in the lattice unit. For the former, six values of up and down quark masses $m_{\mathrm{ud}} = 0.002, 0.015, 0.025, 0.035, 0.050$, and 0.080 are taken. For the latter, five values $m_{\mathrm{ud}} = 0.015, 0.025, 0.035, 0.050$, and 0.100 are

used. The smallest value $m_{\mathrm{ud}} = 0.002$ roughly corresponds to 3 MeV in the physical unit, with which pions are in the ϵ regime. In order to investigate the finite volume scaling, we also simulate on a $24^3 \times 48$ lattice with one choice of the sea quark masses $m_{\mathrm{ud}} = 0.025$ and $m_s = 0.080$.

In the hybrid Monte Carlo (HMC) updates, the global topological charge Q of the gauge field is fixed to its initial value by introducing extra (unphysical) Wilson fermions, which have a mass of cutoff order [16]. In our main runs, we set $Q = 0$. We also simulate another sector of topological charge $Q = 1$ at $m_{\mathrm{ud}} = 0.015$ and $m_s = 0.080$.

We accumulate 2500 HMC trajectories for the main runs in the p regime, 4750 (but the trajectory length is 0.5) for the ϵ regime lattice, 1800 for the $Q = 1$ run, and 1900 on the $24^3 \times 48$ lattice. Eighty pairs of low-lying eigenvalues of the massless overlap operator D are computed at every 5 (or 10 in the $Q = 1$ and $L = 24$ runs) trajectories. For the comparison with ChPT, every complex eigenvalue λ^{ov} is projected onto the imaginary axis as $\lambda \equiv \mathrm{Im}\lambda^{\mathrm{ov}}/(1 - \mathrm{Re}\lambda^{\mathrm{ov}}/(2m_0))$. Here $m_0(= 1.6)$ is a parameter to define the overlap-Dirac operator. In the analysis, we consider positive λ only. The integrated autocorrelation time of the lowest λ is measured as 6–24 trajectories depending on the simulation parameters. The statistical error is estimated by the jackknife method after binning data in every 100 trajectories. Details of the numerical simulation will be reported elsewhere.

At each set of sea quark masses, the formula (1) is described by two unknown quantities Σ_{eff} and F. Note that Σ in (3) can be replaced by Σ_{eff} neglecting higher order effects. We first determine these parameters from the lattice data of $\rho_Q(\lambda)$. Roughly speaking, the height of $\rho_Q(\lambda)$ near $\lambda = 0$ determines Σ_{eff} according to the Banks-Casher relation, while the shape in the bulk region is controlled by F, as far as λ is in the region of convergence of the chiral expansion.

Figure 1 shows the spectral density $\rho_Q(\lambda)$ multiplied by π (left panel) and the mode number below λ, $N_Q(\lambda) \equiv V \int_0^\lambda d\lambda' \rho_Q(\lambda')$ (right), calculated at $m_{\mathrm{ud}} = 0.015$ and
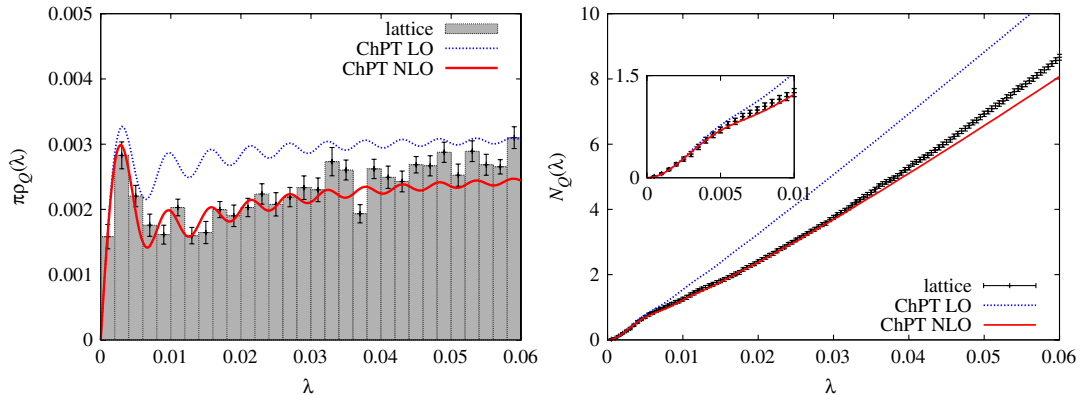

FIG. 1 (color online). Spectral density $\pi\rho_Q(\lambda)$ (left) and mode number $N_Q(\lambda)$ (right) of the Dirac operator at $m_{\mathrm{ud}} = 0.015$, $m_s = 0.080$ and $Q = 0$. The lattice result [given by histogram (left) or solid symbols (right)] is compared with the ChPT formula (1) drawn by solid curves. For comparison, the prediction at the leading order of ϵ-expansion (dashed curves) is also shown.
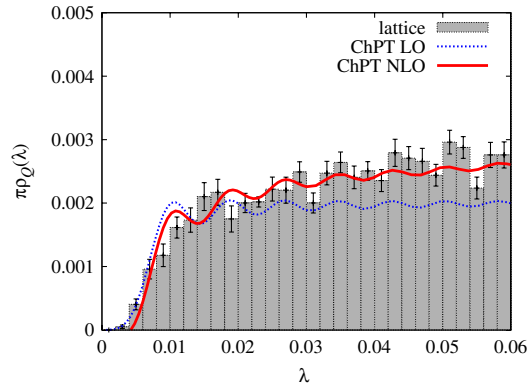
FIG. 2 (color online).   Same as the left panel of Fig. 1, but calculated on the ϵ regime lattice, at $m_{ud} = 0.002$ and $m_s = 0.080$.

$m_s = 0.080$. The solid curve represents the ChPT result (1) with Σ_{eff} and F determined from $N_Q(\lambda)$ at two reference points $\lambda = 0.004$ (~ 7 MeV) and 0.017 (~ 30 MeV). We observe that the formula (1) describes the lattice data well in the region below $\lambda \sim 0.03$ ($\sim m_s/2$) The result is stable within statistical error under changes of the reference points in the range $\lambda < 0.03$. Beyond this value, higher order effects may become larger as suggested in the analysis of the pion mass and decay constant [17]. In the same figure, we also draw the first term of (1). Its discrepancy from the lattice data for $\lambda \gtrsim 0.01$ indicates that the second term $\rho^p(\lambda, \{m_{sea}\})$ in (1) is important for the consistency between QCD and ChPT.

Results from the ϵ regime run are shown in Fig. 2. Σ_{eff} and F are determined from reference points $\lambda = 0.01$ and 0.02. We observe a good agreement between the data and NLO ChPT. The NLO correction is less significant than that in the p regime, but still visible above $\lambda \sim 0.02$.

The values of Σ_{eff} and F are summarized in Table I for all parameter choices. We use the ChPT formulas of both $N_f = 2$ and $2 + 1$ cases. The $N_f = 2$ ChPT formula is understood as the leading contribution in an expansion in

TABLE I.   Numerical results for Σ_{eff} and F. The upper half is the data at $m_s = 0.080$ while the lower is at 0.100.

	$N_f = 2 + 1$ formula		$N_f = 2$ formula	
m_{ud}	Σ_{eff}	F	Σ_{eff}	F
0.002	0.00204(8)	0.0465(100)	0.00204(6)	0.0423(49)
0.015	0.00314(18)	0.0536(15)	0.00305(17)	0.0551(16)
0.025	0.00333(18)	0.0624(20)	0.00326(18)	0.0647(20)
0.035	0.00404(39)	0.0636(17)	0.00393(36)	0.0666(16)
0.050	0.00423(22)	0.0696(16)	0.00413(21)	0.0738(16)
0.080	0.00375(13)	0.0744(15)	0.00367(12)	0.0799(15)
0.015	0.00309(14)	0.0564(19)	0.00303(13)	0.0578(19)
0.025	0.00349(20)	0.0622(17)	0.00342(19)	0.0642(17)
0.035	0.00418(40)	0.0647(14)	0.00409(38)	0.0673(14)
0.050	0.00383(13)	0.0713(16)	0.00376(13)	0.0747(16)
0.100	0.00370(13)	0.0770(15)	0.00363(12)	0.0825(15)

terms of the large strange quark mass. Σ and F in this framework depend on the strange quark mass. The curves in Figs. 1 and 2 are drawn using the $N_f = 2 + 1$ formula, but the difference from $N_f = 2$ is hardly visible in the range $\lambda < 0.03$. The numerical results of Σ_{eff} and F are, in fact, insensitive to the choice of N_f in the formula, except for F in the heavy mass region. We also note that there is no significant difference of Σ_{eff} between $m_s = 0.080$ and 0.100, which confirms decoupling of the strange quark from the low-energy dynamics.

From the data in the nontrivial topological sector $Q = 1$, we observe that the topological charge Q largely affects the spectral density near $\lambda \simeq 0$, but the values of $\Sigma_{eff} = 0.00354(48)$ and $F = 0.0521(25)$ are consistent with those at $Q = 0$. The data at $L = 24$ also show the expected scaling behavior from (1). Since the definition of Σ_{eff} (4) explicitly contains the lattice volume, the results from different volumes cannot be compared directly. After converting the $L = 24$ lattice result $\Sigma_{eff} = 0.003\,06(7)$ to that of $L = 16$, we obtain $0.003\,41(18)$, which is consistent with $0.003\,33(18)$ obtained on the $L = 16$ lattice.

Next, we analyze the sea quark mass dependence of Σ_{eff} from which Σ, F and L_6 can be determined. To see the convergence of the chiral expansion, we carry out fits using four, five and six lightest data points as a function of m_{ud} with m_s fixed at 0.080. The data points and fit curves of the $N_f = 2 + 1$ formula are shown in Fig. 3. The curvature due to the chiral logarithm in (4) is manifest.The fit result for Σ^{phys}, which is Σ_{eff} in the limit of $V = \infty$ and $m_{ud} = 0$ while keeping m_s fixed at 0.08, is stable under change of the fitting range. Since we observe no sizable m_s dependence (see Table I), Σ^{phys} can be considered as the one at the physical strange quark mass. From the five points fit, we obtain $\Sigma^{phys} = 0.001\,86(10)$, $F = 0.0406(5)$, and $L_6^r = -0.000\,11(25)$ in the lattice unit, with $\chi^2/dof = 0.7$.

Since F appears starting at the NLO correction in the formula, m_{ud} dependence of the data given in Table I reflects the NNLO effects, which is beyond the scope of this work. A naive linear extrapolation to the chiral limit yields $F = 0.0410(46)$, which roughly agrees with the value from the fit of Σ_{eff}.

Our final result for the chiral condensate Σ^{phys}, in the limit of $m_{ud} = 0$ and m_s fixed at its physical value, is

$$\Sigma^{\overline{MS}}(2 \text{ GeV}) = \left[242(04) \binom{+19}{-18} \text{ MeV} \right]^3, \quad (5)$$

where the errors are statistical and systematic, respectively. The lattice scale $a = 0.1075(7)$ fm is determined from the heavy quark potential $r_0 = 0.49$ fm. We use the nonperturbatively calculated renormalization factor $1/Z_S(2 \text{ GeV}) = 0.806(12)\binom{+24}{-26}$ [18] to convert the result to the $\overline{MS}$ scheme at 2 GeV.

Possible systematic errors are listed in Table II. The error from chiral fit is estimated by taking variations of the fitting range and the choice of N_f in the ChPT formula. Finite volume effect is estimated by taking the difference
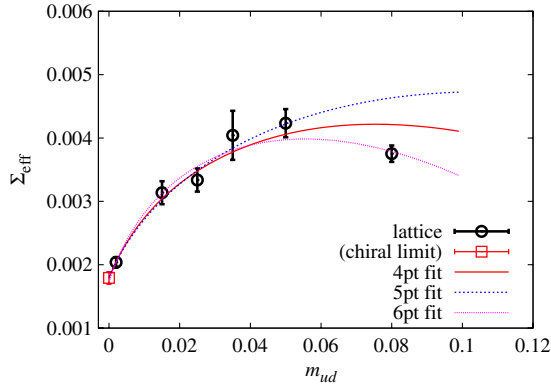
FIG. 3 (color online).   Three parameter fit of Σ_{eff} to the $N_f = 2 + 1$ ChPT.

between the data on $16^3 \times 48$ and $24^3 \times 48$ lattices. The discretization effect is hard to estimate within the calculation done at a single lattice spacing, but partly reflected in the mismatch of the lattice spacing obtained from different inputs: 0.100(5) fm from the pion decay constant [19] and 0.109(2) fm from the Ω baryon mass [20]. To be conservative, the maximum deviation from the central value ($\sim 7.4\%$) is added in both positive and negative directions in Table II.

The chiral condensate obtained in this work (5) is consistent with other determinations from the pseudoscalar meson mass, $\Sigma^{\overline{\text{MS}}}(2 \text{ GeV}) = [257(14) \text{ MeV}]^3$ [19] and from the topological susceptibility, $\Sigma^{\overline{\text{MS}}}(2 \text{ GeV}) = [249(4) \text{ MeV}]^3$ [21,22]. The former is obtained with the NNLO ChPT formula, while the latter only uses the LO relation (and the errors do not contain the systematic effects). Our result is also consistent with two-flavor results in the previous works [1,2,12,17,23,24]. Namely, there is no significant effect of the strange sea quark.

We also obtain $F = 74(1)(8)$ MeV and $L_6^r(770 \text{ MeV}) = -0.00011(25)(11)$. Their systematic errors are estimated in a similar manner.

By the use of the eigenvalue density of the Dirac operator calculated on the lattice, the chiral condensate is determined without suffering from large subtraction of ultraviolet divergences. The dependence on the volume, topological charge and quark masses is well described by ChPT at NLO in the region where both λ and m_{ud} are smaller than $m_s/2$.

TABLE II.   Systematic errors for $[\Sigma^{\text{phys}}(2 \text{ GeV})]^{1/3}$. The total error is obtained by adding each estimate by quadrature.

renormalization	$^{+1.2}_{-1.1}\%$
chiral fit	$^{+2.2}_{-0.7}\%$
finite volume	$^{+1.4}_{-0.0}\%$
finite a	$\pm 7.4\%$
total	$^{+7.9}_{-7.5}\%$

[1] H. Fukaya *et al.* (JLQCD Collaboration), Phys. Rev. Lett. **98**, 172001 (2007).
[2] H. Fukaya *et al.* (JLQCD and TWQCD Collaborations), Phys. Rev. D **76**, 054503 (2007).
[3] H. Neuberger, Phys. Lett. B **417**, 141 (1998).
[4] H. Neuberger, Phys. Lett. B **427**, 353 (1998).
[5] T. Banks and A. Casher, Nucl. Phys. **B169**, 103 (1980).
[6] P. H. Damgaard and S. M. Nishigaki, Nucl. Phys. **B518**, 495 (1998).
[7] T. Wilke, T. Guhr, and T. Wettig, Phys. Rev. D **57**, 6486 (1998).
[8] G. Akemann and P. H. Damgaard, Nucl. Phys. **B528**, 411 (1998).
[9] P. H. Damgaard and S. M. Nishigaki, Phys. Rev. D **63**, 045012 (2001).
[10] T. DeGrand, Z. Liu, and S. Schaefer, Phys. Rev. D **74**, 094504 (2006) **74**, 099904 (2006); C. B. Lang, P. Majumdar, and W. Ortner, Phys. Lett. B **649**, 225 (2007); P. Hasenfratz, D. Hierl, V. Maillart, F. Niedermayer, A. Schafer, C. Weiermann, and M. Weingart, J. High Energy Phys. 11 (2009) 100.
[11] P. H. Damgaard and H. Fukaya, J. High Energy Phys. 01 (2009) 052.
[12] L. Giusti and M. Luscher, J. High Energy Phys. 03 (2009) 013.
[13] J. C. Osborn, D. Toublan, and J. J. M. Verbaarschot, Nucl. Phys. **B540**, 317 (1999).
[14] P. Hasenfratz and H. Leutwyler, Nucl. Phys. **B343**, 241 (1990).
[15] J. Gasser and H. Leutwyler, Ann. Phys. (Leipzig) **158**, 142 (1984); Nucl. Phys. **B250**, 465 (1985).
[16] H. Fukaya *et al.* (JLQCD Collaboration), Phys. Rev. D **74**, 094505 (2006).
[17] J. Noaki *et al.* (JLQCD and TWQCD Collaborations), Phys. Rev. Lett. **101**, 202004 (2008).
[18] J. Noaki *et al.* (JLQCD Collaboration), arXiv:0907.2751.
[19] J. Noaki *et al.* (JLQCD and TWQCD Collaborations), Proc. Sci. LAT2009 (2009) 096.
[20] J. Noaki *et al.* (JLQCD and TWQCD Collaborations) to be published.
[21] T. W. Chiu *et al.* (JLQCD and TWQCD Collaborations), arXiv:0810.0085.
[22] T. W. Chiu, T. H. Hsieh, and P. K. Tseng (TWQCD Collaboration), Phys. Lett. B **671**, 135 (2009).
[23] S. Aoki *et al.* (JLQCD and TWQCD Collaborations), Phys. Lett. B **665**, 294 (2008).
[24] H. Fukaya *et al.* (JLQCD Collaboration), Phys. Rev. D **77**, 074503 (2008).